Article

Hardware in the Loop Real-Time Simulation for Heating Systems: Model Validation and Dynamics Analysis

Wessam El-Baz* [1], Lukas Mayerhofer[1], Peter Tzscheutschler [1] and Ulrich Wagner [1]

[1] Institute of Energy Economy and Application Technology, Technical University of Munich. Arcisstr. 21 80333 Munich, Germany

* Correspondence: wessam.elbaz@tum.de; Tel.: +49-(0)89-289-28314

Abstract: Heating systems such as heat pump and combined heat and power cycle systems (CHP) are representing a key component in the future smart grid. Their capability to couple the electricity and heat sector promises a massive potential to the energy transition. Hence, these systems are continuously studied numerical and experimental to quantify their potential and develop optimal control methods. Although numerical simulations provide time and cost-effective solution for system development and optimization, they are exposed to several uncertainties. Hardware in the loop (HiL) system enables system validation and evaluation under different real-life dynamic constraints and boundary conditions. In this paper, a HiL system of heat pump testbed is presented. This system is used to present two case studies. In the first case, the conventional heat pump testbed operation method is compared to the HiL operation method. Energetic and dynamic analyses are performed to quantify the added value of the HiL and its necessity for dynamics analysis. The second case, the HiL testbed is used to validate the heat pump operation in a single family house participating in a local energy market. It enables not only the dynamics of the heat pump and the space heating circuit to be validated but also the building room temperature. The energetic analysis indicated a deviation of 2% and 5% for heat generation and electricity consumption of the heat pump, respectively. The model dynamics emphasized the model capability to present the dynamics of a real system with a temporal distortion of 3%

Keywords: Modelica; Heat pump; HiL; Model Validation;Testbed

0. Introduction

Installed renewable energy capacities are growing fast worldwide. At the end of 2017, 2179 GW were installed, with a growth rate of 8.3% during 2017 [1,2]. These capacities are expected to continue growing to minimize the CO_2 emissions and mitigate the climate change. In Germany, several legislations were introduced to create a nuclear and fossil-free economy within the framework of the energy transition[3]. Among these acts are the renewable energy act, Erneuerbare Energien Gestez (EEG), and the combined heat and power act, Kraft-Wärme-Kopplungsgesetz (KWKG). The EEG prioritizes the renewable energy sources (RES) in the energy market [4]. It guarantees a fixed feed-in tariff for the supplier to minimize the risk of the investors. Hence, the RES reached 111 GW in 2017 [4]. On the other hand, KWKG empowers the integration of combined heat and power (CHP) systems in the national grid. A goal was set to generate 25% of the electricity by co-generation by 2020 [5]. As these two acts increased the renewable energy capacities and increased the system efficiency, they raised several challenges in the national grid and made the traditional grid management techniques rather obsolete.

Sector coupling is one way to address these challenges faced by the grid. Heat pumps and CHP systems are the key drivers behind the electricity and heat sectors coupling. The attractive costs and lifespan of heat storages enable these heating systems to be more economically feasible to offer flexibility and mitigate the fluctuating RES. Furthermore, the continuous improvement of the heat pumps coefficient of performance (COP) over the past decades [6] led to a significant decrease in the operation and maintenance costs. On the other hands, CHP systems are available in the markets at multiple scales to serve different the utility and prosumers.

Given these heating systems potential in the current and future national energy system, several researchers modeled and studied these heating systems [7–11]. Although the presented heating system models can predict to a good extent the energy generation or consumption of a real-system, they are exposed to several uncertainties as they are designed to be integrated into larger models under specific system constraints. Hence, testbeds and field tests were used to investigate the quality of the result and analyze the real-life system dynamics.

Hardware in the loop (HiL) is an approach to simulate and evaluate thermal system dynamics under multiple environmental constraints. The fundamental idea of the HiL is to integrate real hardware in a simulation loop. Real hardware replaces mathematical model of a system to study and evaluate the quality of a developed control or optimization algorithm [12]. Hardware can also be integrated with multiple numerical models to investigate its reaction to model combinations. As an example, a HiL system of a heat pump as hardware and a controller as software can be used to evaluate the quality of the control system. Also, a building model can be integrated to show the heat pump dynamics and reaction to different building types, ages, or sizes.

In the literature, HiL simulation is being used in several fields. According to [12,13], it has been used for over 50 years. An early application was in the flight and missiles control industry as in the Sidewinder program in 1972 [14]. It has also become more popular in other industries. As an example, HiL represents nowadays a crucial tool in the automotive industry [13,15]. It is extensively used for engine and suspension systems control and design. Moreover, Hil is used also for testing unmanned aerial vehicles as in [16]. In the electrical power sector, applications of HiL for testing and validating are growing. [17] used a HiL system to study the dynamic performance of a switch-mode power amplifier. In [18] a power HiL system was introduced and used to evaluate a case study of a Great Britain network. [19] implemented a HiL system to investigate and compare the performance of multiple control techniques for Single-Ended Primary Inductance converter(SEPIC). [20] investigated different energy management strategies with electric vehicles using a HiL system in real-time. The author's setup facilitated the evaluation of the effectiveness of the design EMS strategies in real-time. Furthermore, [21] designed a HiL system for water electrolysis system emulation. Through this system, the author was able to study the electrolyzer characteristics in a smart grid. In [22], voltage control coordination scenarios were validated based on a HiL system. The authors used HiL in a real-time simulation to validate the capability of RES to provide voltage control in a smart grid.

Although several publications are available for power HiL systems, a limited number of publications are discussing the heating systems in buildings. Among these publications is the work of [23], where a HiL simulation system was developed to evaluate the control strategies of a hydronic radiant heating system. The author replaced the model of the hydronic network with real hardware to minimize the results uncertainties. In [24], a HiL system was developed to simulate micro-CHP systems with different building models. The author showed the necessity of a HiL system in the operation of micro-CHP testbeds and evaluation of optimization and control algorithms.

At the Institute of energy economy and application technology (IfE), several testbeds were developed to evaluate all the common heating systems at different scales as in [25–27] and recently in [28]. A testbed is necessary to demonstrate and validate the novel optimization algorithms and control strategies being developed. Through these testbeds the operational requirements and technical constraints were easily defined. Ideally, a heating system testbed should be able to demonstrate and emulate a real building with a heating system and is expected to eliminate all the uncertainties, as real

Peer-reviewed version available at Energies 2018, 11, 3159; doi:10.3390/en11113159

hardware is used. However, as the buildings are emulated by heat sinks, uncertainties can emerge and the building dynamics in certain cases diminish. The HiL systems developed at the IfE presented in [24] showed the preliminary results, the potential of the HiL system, and basic evaluation of the uncertainties that can emerge during the simulation. Using the recent advanced HiL version of [24], the testbed in [28]and model presented in [29], the following aspects are demonstrated:

- A comparison between heating systems testbeds operation with HiL and without HiL system simulation
- An energetic and dynamics analysis to quantify the benefits of HiL simulation with heating systems
- A model validation of the heat pump dynamics and interactions within a microgrid in an energy market.

The structure of the paper is as follows: Section 1 shortly describes the different numerical and experimental methods used to analyze a heating system. Section 2 demonstrates the HiL system structure including the testbed and the building model. Moreover, it presents the input system parameters. Section 3 demonstrates and discusses the results of the two cases discussed in this publication. Section 4 presents a conclusive summary of the whole study.

1. Heating Systems Analysis Methods

Numerical simulation provides the ideal environment for testing and evaluation of a heating system performance connected to different buildings types. Compared to experimental testing, it saves efforts, costs and time to investigate a specific heating system. However, it is exposed to several uncertainties, and its accuracy is questionable. Hence, experimental evaluation has always an edge over the numerical simulation as it eliminates the modeling uncertainties.

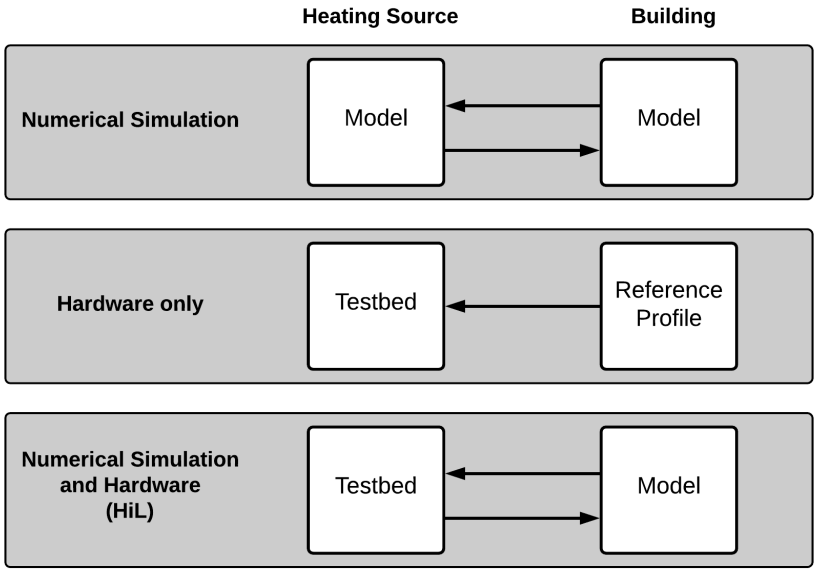

Figure 1. Abstract diagram of different methods for heating system analysis

The experimental testing can only be performed using hardware, or hardware and numerical models as HiL. Figure 1 presents an abstract comparison between heating system analysis using numerical simulation, hardware only (without HiL), and hardware and models (HiL). The conventional method to evaluate the heating system experimentally is using hardware only. A reference profile that

Preprints (www.preprints.org) | NOT PEER-REVIEWED | Posted: 26 October 2018 doi:10.20944/preprints201810.0632.v1

Peer-reviewed version available at Energies 2018, 11, 3159; doi:10.3390/en11113159

is obtained within a field test or by a simulation model is fed directly to the testbed. This reference profile contains the thermal load of the building P_{th} over a specific period of time. The testbed hydraulic circuit emulates this load profile using a heat sink to evaluate the reaction of the heat source and heat storage. Although the heating source such as a heat pump or a micro-CHP system is a real system, the results of the whole experiment are exposed to uncertainties because of the heat sink emulation of the reference load profile. The heat sink always tries to reach the set reference profile, even if it has to decrease the return temperature to or below the room temperature. As a conventional alternative solution, return temperature can be held constant, yet it diminishes the dynamics of the whole testbed operation.

A combination of hardware and numerical simulation is considered ro be the optimal method for heating systems analysis and models validation. The heating source and heat storage are integrated as a hardware with a building model using a HiL system to evaluate and validate heating systems dynamics and performance. Consequently, the building model can calculate realistic return temperatures and the feedback of the building for any violation introduced by the heating source. Furthermore, the room temperature can be simulated by the building model. Hence, the user comfort can be analyzed in real-time.

2. HiL Simulation System

2.1. Communication Structure

Figure 2 shows the detailed control loop of the implemented HiL model. The heat pump (HP) controller, temperature controller, building model, and the tapping profiles are implemented on SimulationX, which is a Modelica based software. More details about the models are explained later in this section. The testbed, the hardware, is presented by three modules: heat sink, heat storage, and heat source, which are the typical components of a heating system testbed. A LabVIEW program controls the different components of the testbed and feeds the output to the database.

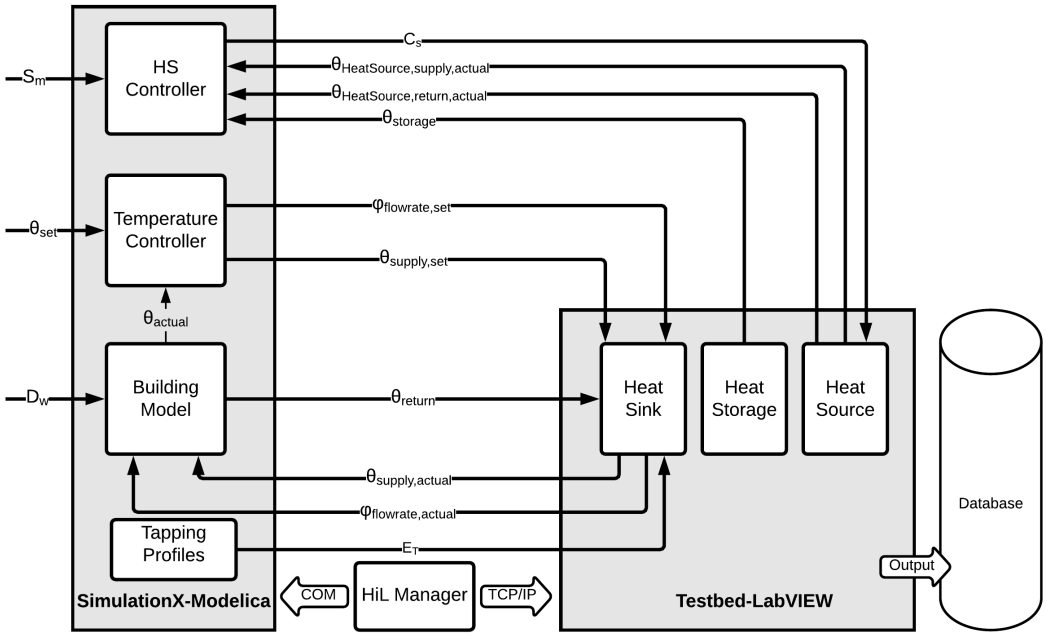

Figure 2. Detailed control diagram of the HiL system

The communication between the model in SimulationX and LabVIEW is managed by the HiL manager, which is based on a Matlab Code. The data is transferred between the HiL manager and the LabVIEW based on the TCP/IP protocol, while a COM interface is used to manage the SimulationX simulation. The details of the HiL manager communication protocols and steps are thoroughly documented in [24].

Other communication systems were tested such as exporting the building models in the C programming language (C-code) and importing the model in LabVIEW. However, processing the C-code in real-time desynchronize the LabVIEW real-time control. Moreover, the number of inputs and outputs to and from the C-code are limited. Hence, using C-code for integrating models in real-time LabVIEW control systems is not be feasible for heating systems applications, given the size of C-code and the number of communicated variables.

The communicated data between the testbed and the SimulationX models is dependent on the functionality of the model and testbed module. The HS controller receives the actual heat source supply temperature $\theta_{HeatSoruce,supply,actual}$, actual heat source return temperature $\theta_{HeatSoruce,return,actual}$, and temperature of the storage $\theta_{storage}$ from the testbed. Moreover, it receives an external control input signal S_m that is developed from the model described in [29]. Based on these input signals, the HS controller sends a binary operation signal C_s to the testbed heat source. The temperature controller receives θ_{set} and θ_{actual}, which are the set room temperature and the actual room temperature, respectively. Based on these two inputs, the temperature controller can calculate the set flow rate $\varphi_{flowrate,set}$, and the set space heating supply temperature of the $\theta_{supply,set}$. The building model receives the weather data D_w, actual flow rate $\varphi_{flowrate,actual}$, and the actual supply temperature of the space heating $\theta_{supply,actual}$. Based on these inputs and the building model, the return temperature can be calculated and forwarded to the testbed. Communicating the θ_{return} each second in this HiL simulation system maximizes the results accuracy and enables the testbeds to present realistic dynamics that is comparable to field measurements. Tapping profiles can also be integrated as a model and communicated as energy profiles E_T to the heat sink.

2.2. Testbed Components and description

The testbed system consists of three modules and a brine water heat pump with a thermal power of 10.31 kW and a COP of 5.02 by B0/W35 as per standard EN14511. Two circulations pumps are integrated into the heat pumps on the brine and the water side. Moreover, it is equipped with an emergency electrical heater of 8.8 kW. Figure 3 shows the simplified hydraulic schematic of the used testbed.

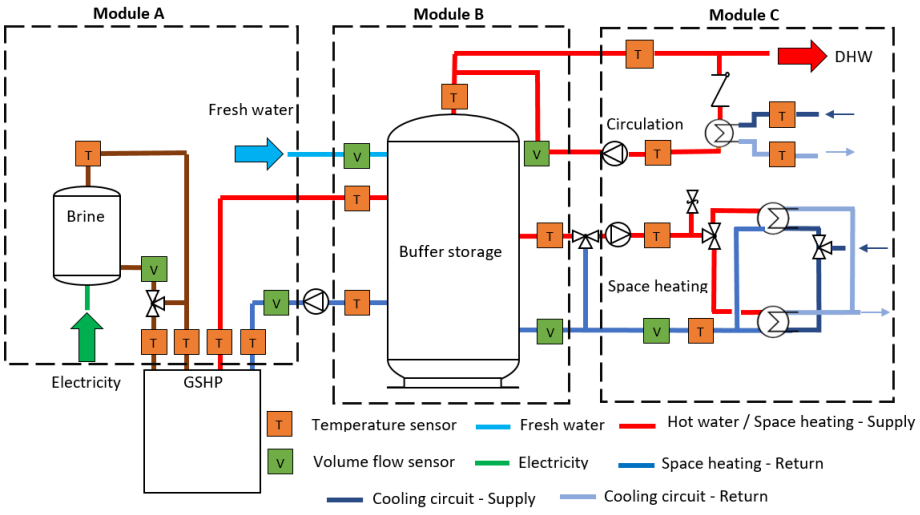

Figure 3. Hydraulic schematic of the heat pump testbed [28]

Having a ground-source heat pump, an emulator is needed to show the dynamics of the ground heat exchanger. Module A includes a ground-source emulator that can emulate any required brine temperature supplied to the heat pump. It consists of a 300-liter heat storage, filled with a water-glycol mixture as an anti-freezing heat transfer fluid. The storage is heated by a 12.5 kW electrical heater that is controlled via a hysteresis regulator to maintain the tank temperature during the whole operation time at 40 °C. The set temperature of the tank and the hysteresis bandwidth can be defined by the user depending on the simulation goals. A mixer, similar to the conventional space heating mixers, is used to mix the supply of brine tank with the return of the heat pump to reach the required ground-source set temperature. Depending on the HiL system and the goal of the simulation, the mixer can maintain a constant brine temperature or a time-dependent temperature profile.

Module B shows the combi-storage system of a conventional residential house. It includes a 749-liter combi hygienic buffer storage to cover the space heating and domestic hot water consumption. A stainless steel heat exchanger extracts heat from the storage to cover the hot water consumption. Moreover, a coaxial pipe, pipe-in-pipe system, is used to enable the hot water and maintain the pipe temperatures at a certain level.

Module C is the most complex module as it represents the heat sink of the testbed. It can emulate the space heating and domestic hot water consumption depending on the building type and user behavior. The space heating circuit consists of a space heating mixer, circulation pump, and two heat exchangers. Through the mixer, the supply of the tank with the return of the space heating is mixed to reach the required $\theta_{supply,set}$. The circulation pump is controlled depending on $\varphi_{flowrate,set}$, which varies depending on the heat demand. Two heat exchangers of two different sizes are used to emulate different building loads depending on their required maximum heat power. The domestic hot water consumption is emulated through three magnetic valves that have different consumption flow rates. These valves can represent different consumption activities such as washing, showering or cooking.

The hydraulic configuration in figure 3 shows only one of the most common hydraulic configuration. However, the testbed can allow several other configurations, such as the direct connection of the heat pump to module C, or using an additional heat storage for hot water consumption. More details about the hydraulics, control and dynamics of the testbed are available in [28].

2.3. Models Description

Earlier in [29], a market model is presented based on a double-sided auction, in which different household devices and heating systems can participate. The heat system bids their energy needs to either minimize their costs, maximize comfort, or local generation in a microgrid. In this paper, the market control approach is going to be used to develop the external control signal, S_m. The control signal provided in this case is a binary signal, either 0 or 1. The HS controller reacts to the signal as in equation 1, where $\theta_{HeatSource,supply,max}$ is the maximum heat source supply temperature, $\theta_{HeatSource,return,max}$ is the maximum heat source return temperature, and $\theta_{storage,max}$ is the maximum storage temperature at a specified sensor position.

$$C_S = \begin{cases} 0, & \text{if } \theta_{HeatSource,supply,actual} \geq \theta_{HeatSource,supply,max}, \\ 0, & \text{if } \theta_{HeatSource,return,actual} \geq \theta_{HeatSource,return,max}, \\ 0, & \text{if } \theta_{storage} \geq \theta_{storage,max}, \\ S_m, & \text{otherwise} \end{cases} \tag{1}$$

The S_m is considered in full control, yet the HS has to make sure that the heat source operation never exceeds the operation limit set by the manufacturer.

The temperature controller sets the flow rate and supply temperature of the heating circuit. The flow rate is determined based the room actual temperature θ_{actual} and set temperature θ_{set}, while the supply temperature is determined based on the outside temperature in D_w. To control the flow rate,

the temperature controller operates based on a hysteresis algorithm. The set flow rate of the heating circuit $\varphi_{flowrate,set}$ is calculated based on $\theta_{actual} - \theta_{set}$, Δ_r^+, and Δ_r^- where Δ_r^+ and Δ_r^- are the hysteresis upper and lower limits, respectively. These limits are determined by the user depending on the level of comfort required. The smaller the absolute value of Δ_r^+ and Δ_r^-, the higher comfort. Equation 2 details the control cases of the flow rate.

$$\varphi_{flowrate,set} = \begin{cases} \varphi_{flowrate,min}, & \text{if } \theta_{actual} - \theta_{set} > \Delta_r^+, \\ \varphi_{flowrate,max}, & \text{if } \theta_{actual} - \theta_{set} < \Delta_r^-, \\ \dfrac{\varphi_{flowrate,max} - \varphi_{flowrate,min}}{\Delta_r^+ - \Delta_r^-} \times (\theta_{actual} - \theta_{set}) + \varphi_{flowrate,min}, & \text{otherwise} \end{cases} \tag{2}$$

The supply temperature is determined based on the outside temperature given in D_w. The supply temperature varies linearly against the outside temperature. The lower the outside temperature, the higher is the supply temperature of the space heating system. The limits and the magnitude of this linear relationship between the outside temperature and the heating system supply temperature is defined based on the age of the building and the type of the radiators. In section 2.4, the used supply temperature curve is explained.

2.4. Model Input Data and Parameters

The building model is created and calibrated based on the research project data of [30]. It consists of three heated zones to represent an Attic, a living area and a cellar. The base model is available in the Green City package of SimulationX [31]. The construction year of the building is between 1984 and 1994. The living area has 150 square meters and a room height of 2.5 meters. The cellar and attic are unheated. The living area is heated and the temperature is maintained at 21 °C. In table 1, a summary of the most important input data parameters are presented.

Table 1. Building and control models basic parameters

Description	Value	Units[-]
Building age	1984-1994	-
Building type	residential	-
Flanking	none	-
Number of occupants	4	-
Heated living area	150	m^2
Clear room height	2.5	m
Body heat dissipation per person	80	Watt
Set temperature - θ_{set}	21	°C
Initial zone temperature	21	°C
Upper hysteresis limit- Δ_r^+	0.5	K
Lower hysteresis limit- Δ_r^-	-0.5	K
Heating system exponent	1.2	-
Max. flow rate - $\varphi_{flowrate,max}$	0.24	l/s
Min. flow rate - $\varphi_{flowrate,min}$	0	l/s
Max. heat source supply temperature - $\theta_{HeatSource,supply,max}$	65	°C
Max. heat source return temperature - $\theta_{HeatSource,return,max}$	55	°C
Max. storage temperature (lowest layer) - $\theta_{storage,max}$	55	°C
Night setback	10	K

A winter cloudy type day is selected based on the VDI Standard 4655. The ambient weather temperature, the global solar irradiation, and the cloudiness are shown in figure 4. According to the standard, the average temperature should be below 5°C and the cloudiness should be higher than 5/8. On the selected day, the average temperature and cloudiness was 3.15°C and 7/8, respectively. The number of cloudy winter days in the reference year was 85 days. The presented profile represents a typical average day of the given year in Munich Germany. A winter type day is chosen to show clearly

Preprints (www.preprints.org) | NOT PEER-REVIEWED | Posted: 26 October 2018 doi:10.20944/preprints201810.0632.v1

Peer-reviewed version available at Energies 2018, 11, 3159; doi:10.3390/en11113159

the influence of HiL on the quality of the results. A summer type day could have been selected, yet the space heating circuit would not be activated in this case. Hence, the HiL influence would not be noticed.

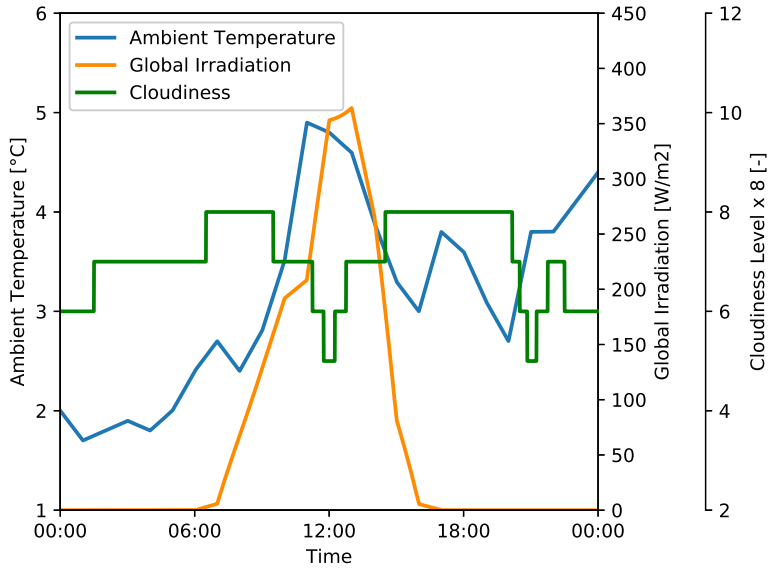

Figure 4. A winter cloudy type day temperature and global irradiation

The heating circuit supply temperature is defined according to equation 3, where θ_a is the ambient temperature. As shown, the supply temperature varies depending on the outside ambient temperature. The slope of the supply temperature is defined according to the recommended operation constraints and the nature of the building itself. Moreover, the required set temperature and required user comfort level can play an important role in deciding the slope of the heating curve. A change in the set temperature or the comfort level can be accompanied by a parallel shift of the heating circuit supply curve. To increase the comfort and the decrease the time required to reach the set temperature, parallel upwards shift can be made. On the other hands, if the user needs to decrease the costs, the heating curve can be shifted downwards.

$$\theta_{Supply,set} = \begin{cases} 50, & \text{if } \theta_a < -20 \\ -0.625 \times \theta_a + 37.5, & \text{if } -20 \leq \theta_a \leq 20, \\ 25, & \text{if } \theta_a > 20 \end{cases} \quad (3)$$

3. Results and Analysis

In this paper, two cases are evaluated. The first case compares the testbed operation with and without HiL to present the added value and necessity of the HiL system. The comparison is based on energetic and dynamics analysis of the two experimental methods. The energetic analysis compares the energy consumption of the heat source and heat sink within the period of time depending on the given type day in section 2.4. The dynamic analysis investigates and compares power and temperatures over time of the two testbed experiments with and without HiL and discusses its impact on the heating system evaluation.

In the second case, the HiL system is used to validate a single family house model with a heat pump participating in an energy market. Preliminary market model was presented in [29]. The system dynamics evaluation of the model is crucial as it influences the time, volume and price of the heat

pump energy asked from the market. Hence, a comparison is conducted between the HiL system and the model to evaluate and demonstrate the model accuracy.

3.1. Case 1: Testbed Operation With and Without HiL

In this case, the testbed operation with and without HiL is compared to quantify the added value and present the necessity of the HiL system. A reference load profile is generated from the building model and type day presented in section 2.4. The building model is connected to an over-sized heating source or a district heating to simulate the exact heat demand profile of the building without any compromises on the comfort side of the user.

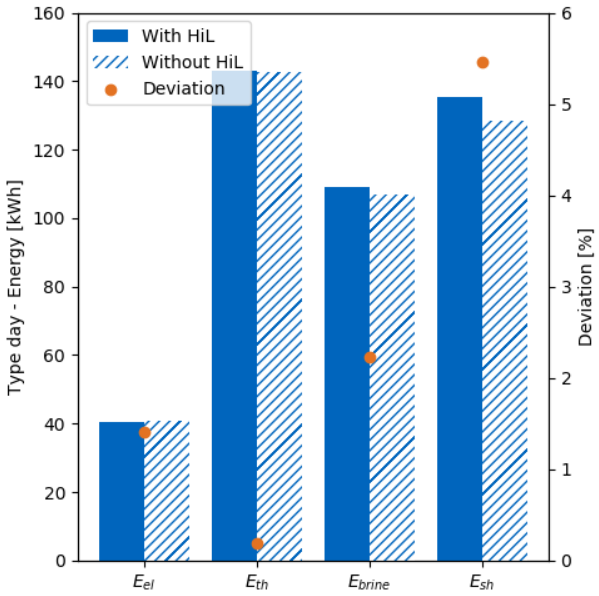

Figure 5. Energetic analysis of the testbed performance with and without HiL

Figure 5 presents the energy consumption and generation of the type day experiment, where E_{el} is the electric energy consumption of the heat pump, E_{th} is the thermal energy generation of the heat pump, E_{brine} is the energy consumed from the brine side, and E_{sh} is the energy consumed by the building. It can be seen that the deviation is between 0.2% to 5.5%, which is not significantly large. However, it can be noticed that using the same metrics, the operation without HiL always has a lower consumption than the one with HiL. The reference space heating profile consumption is 132.8 kWh, compared to 135.3 kWh for the operation with HiL and 128.4 kWh for the operation without HiL. Although the experiment with HiL system is closer to the reference, it does not indicate a significant failure in the experiment without HiL. Hence, operating heating system testbeds without a HiL communication system has been widely accepted over the past years.

Insight on the dynamics and the difference between the testbed operation with and without HiL can be presented in figure 6. Although the energy consumption is almost equal, a significant difference can be seen in the space heating dynamics between the operation with HiL, without HiL and the reference profile. Between 00:00 and 06:00 in figure 6(a), no differences can be noticed. The testbed operations are identical to the reference profile. With the increasing demand after 06:00 and the lack of sufficient energy in the heat storage, the power dropped. The testbed operation without HiL reaction is to reduce the return temperature trying to maintain the same power, as in figure 6(b). The return temperature in this case decreases to 17°C, which shows a major violation as the return temperature is lower than the room temperature. The testbed would have decreased the return temperature even to a lower level than 17°C, but it is constrained by the cooling circuit. On the other hand, the HiL

Preprints (www.preprints.org) | NOT PEER-REVIEWED | Posted: 26 October 2018 doi:10.20944/preprints201810.0632.v1

Peer-reviewed version available at Energies 2018, 11, 3159; doi:10.3390/en11113159

system maintained a plausible return temperature due to the integration of a building model in the loop. Moreover, the HiL increased the power after 08:00 to make up for the power drop started at 06:00 and maintain a proper temperature, while the testbed operation without continued to maintain the reference profile.

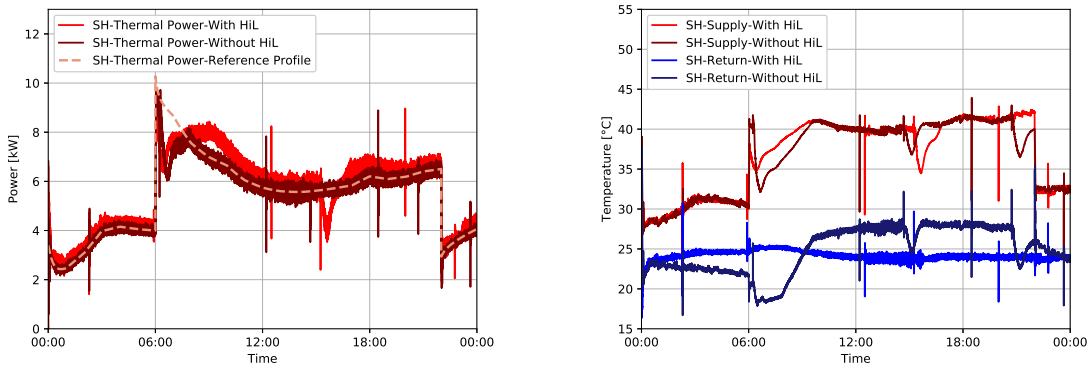

(a) (b)

Figure 6. Comparison between the space heating dynamics of the testbed operation with HiL and without HiL against the reference profile, (a) space heating thermal power, (b) space heating supply and return temperatures

Another drop in power can be noticed between 12:00 and 18:00 for the HiL system. The testbed operating without HiL maintained the reference load profile power, even though there were not sufficient amount of energy in the storage. This can be confirmed by the decrease in supply temperature noticed in figure 6(b). This drop is due to incapability of the heat pump to meet the demand. The HiL maintained a plausible return temperature, but return temperature without the HiL decreased significantly. Although the power of the testbed operation without HiL seems acceptable, the return temperature dynamics are not realistic and can not be relied on for model validation or further research.

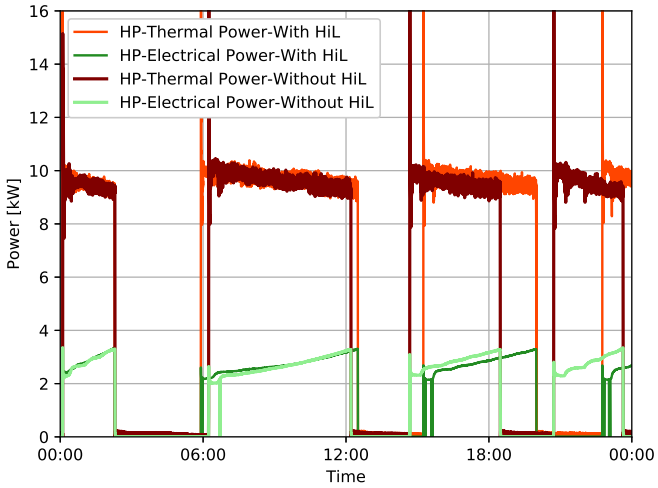

Figure 7. Thermal and electrical power of the heat pump with and without HiL

The energetic analysis shows almost an identical energy consumption and generation behavior of the heat pump system, yet the system dynamics shows the necessity of a HiL system. The behavior of

the space heating circuit led to another operation plan for the heat pump, although it uses the same controller strategy. As in figure 7, the heat pump started at the same time and behaved similarly within the first operation cycle. With the second cycle starting at 06:00, a difference between the two cycles can be seen. This difference is increasing over time as seen at 15:00 and again at 20:00. This difference between the two systems can lead to a significant error in the evaluation of energy management systems using heat pumps and cost optimization models based on variable electricity tariffs, or in energy markets as discussed later in section 3.2. The exact operation plan represents a necessity in evaluating and validating the flexibility potential of heat pumps.

3.2. Case 2: Model Validation Based on HiL

Based on the model presented in [29], 10 single family residential houses are simulated located in Munich, Germany. These houses are participating in a local energy market, where each device sell or buy energy depending on its operation mode. Each house is equipped with a photovoltaic system, an electric vehicle and a heat pump. The installed PV capacity at each house is 6 kWp. The technical details and the data of the integrated PV system can be found in [32]. A 3.6 kW charging station is used for the electric vehicle, while the integrated heat pump is represented by the testbed in section 2.2. More details about the heat pump testbed can be found in [28]. A single family house is selected from these 10 houses to be validated based on the HiL system and the heat pump testbed.

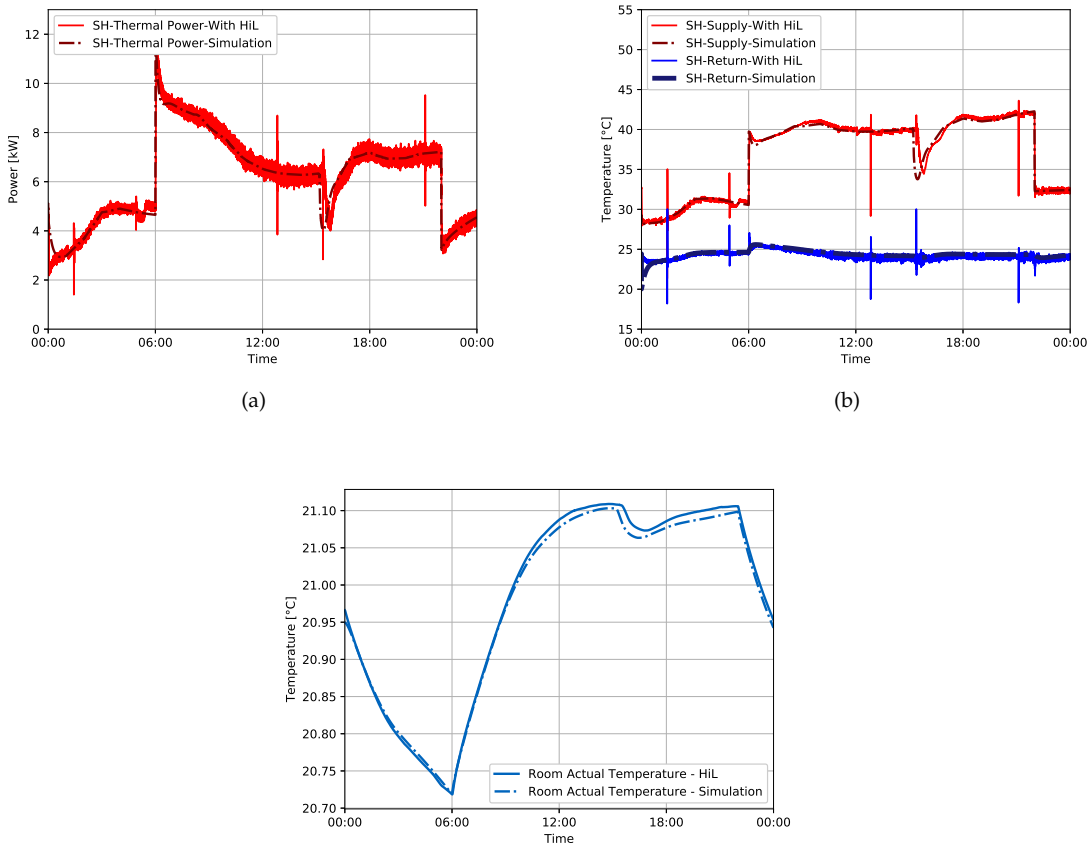

Figure 8. Comparison between the heat pump dynamics of the testbed operation with HiL and simulation, (a) space heating thermal power, (b) space heating supply and return temperatures, (c) room temperature

The goal of the model validation is to compare the operation of the heat pump in the model to the testbed with HiL, while making sure that the building load is covered and the room temperature is properly maintained. On the heat sink side, figure 8(a)shows that the space heating power of the testbed with HiL and the simulation are behaving similarly, even when a drop in the storage energy occurred at 17:00. This drop did not influence the room temperature as shown in figure 8(c). The room temperature of the complete simulation model and the building model within the HiL system are behaving similarly. A difference can be noticed from 09:00 to 22:00, yet this difference is below 0.02 °C. In figure 8(b), the supply and return temperature of the HiL testbed and simulation model can be compared. It can be noticed that the return temperatures are not violated and both the HiL and simulation are behaving similarly except at the starting point, where a minor fluctuation occurred by the simulation solver.

The behavior of the heat pump in the HiL and simulation is almost identical as in figure 9. The power magnitude of the thermal and electrical power is equivalent, which means that the heat pump has been providing power to the heat storage almost at the same supply temperature. In this type day, the energy difference between the HiL system and the simulation is 2% and 5% for the heat generation and electricity consumption, respectively. However, the HiL based validation in this paper is not only concerning the energetic consumption but also the temporal distortion of the power. The time and volume of the heat pump bid in an energy market have to be evaluated to validate the accuracy of the heat pump bid in the market.

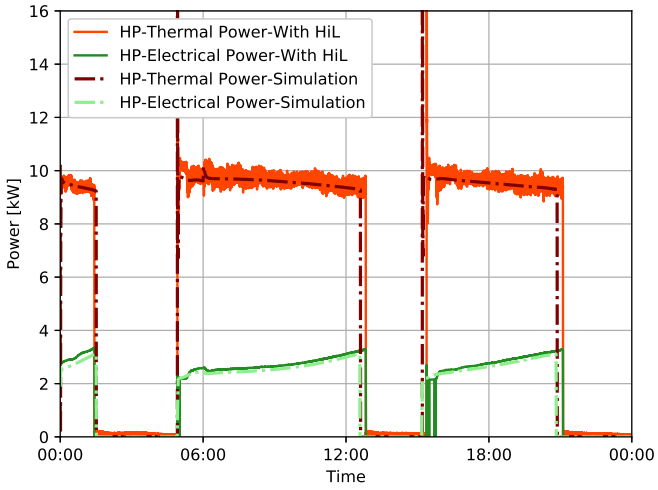

Figure 9. Heat pump thermal power and electrical power on the type day

In [28], the thermal and electrical power of the heat pump model were validated independently based on mean absolute percentage error (MAPE) and root mean square error (RMSD). However, since the temporal distortion of the model compared to the HiL is crucial to evaluate the model capability in participating in local energy markets at the estimated times, the temporal distortion index (TDI) of [33] is used. This metric is based on the dynamic time warping (DTW) developed in the 70s, which is used to evaluate the temporal distortion between two different time series. In this paper, the two time series are the HiL measurement and simulation model time series of the heat pump electrical power. The DTW finds the optimal path through minimizing the distance between the two given time series. Then, it returns the optimal warping path given the simulation model output with the index i, the HiL measurements with the index j, and the smallest distance between them. The TDI is calculated then according to equation 4.

$$TDI = \frac{1}{N^2} \sum_{l=1}^{k-1} |(i_{l+1} - i_l)(i_{l+1} + i_1 - j_{l+1} - j_l)| \quad (4)$$

The output of the TDI is between 0 and 1. The lower the value of the TDI metric, the lower is the temporal distortion. The metric result in this type day is 3%, which means that the simulation model and the HiL have a low temporal distortion.

4. Conclusion

In this paper, hardware in the loop (HiL) real-time system is presented. The HiL communication structure, models and testbeds are explained to show the experimental setup of HiL for heating systems. The testbed of a ground source heat pump (GSHP) demonstrated in [28] is used as a candidate for this study. To evaluate the potential and applications of the HiL, two case studies are discussed. The first case study evaluates the energy consumption and the dynamics of the testbed operation with and without HiL. The results of the case study are summarized as follows:

- Testbed operation with or without HiL does not influence the energy consumption of the heat sink (space heating), or the heat generation from the heat pump. The variations in results are between 0.2% and 5.5%. Hence, energetically no significant difference can be noticed
- The dynamics of the testbed operation without HiL showed that a drop in the space heating supply temperature is always accompanied with a drop in the return temperature of the space heating. Thus, testbed operation without HiL can not emulate real-life return temperature dynamics and can lead to system violations
- The HiL system is able to maintain realistic dynamics due to the availability of a building model in the loop
- The violations of the testbed operation without HiL led to a shift in the operation plan of the heat pump. Hence, the testbed operation without HiL is not reliable for heating system models validation

In the second case, the HiL system was used to validate a single family house building participating in a local energy market. The HiL system was chosen as it was necessary to validate not only the energy consumption but also the system dynamics and the temporal distortion of the model. The simulation model showed its capability to present the heat pump system dynamics including any drops in the supply temperature or the heat storage of the tank. The HiL also showed an advantage of demonstrating the room temperature of the building model for the given type day, which facilitates evaluating the comfort of the residents and comparing it to the simulation model. Furthermore, TDI is used to quantify the temporal distortion of the heat pump to make sure that the electric energy consumption is communicated at the right time of the day. The TDI value is 3%. Hence, a minimal temporal distortion can be noticed between the HiL and the simulation model.

As an outlook, HiL for heating systems can be used for several further studies. It enables not only an accurate validation of simulation model but also experimentation using the building model inertia to offer flexibility to the grid. The HiL can also include not only one heating system or a building model, but also multiple heating systems that can communicate and interact in the same local heating network or a microgrid.

5. Acknowledgment

This work was supported by the German Research Foundation (DFG) and the Technical University of Munich within the Open Access Publishing Funding Program. The research project is supported by the Federal Ministry for Economic Affairs and Energy, Bundesministerium für Wirtschaft und Energie, as a part of the SINTEG project C/sells. Responsibility for the content of this publication lies on the authors.

6. Author Contributions

Wessam El-Baz designed the experiments and developed the HiL system. Lukas Mayerhofer operated the testbed and prepared the energetic analysis. Peter Tzscheutschler and Ulrich Wagner provided a detailed critical review. All the authors discussed the documents results and contributed to the preparation of the manuscript.

7. Conflicts of Interest

The authors declare no conflict of interest

References

1. IRENA International Renewable Energy Agency. Renewable capacity highlights **2018**. p. 2.
2. Capuano, L. International Energy Outlook 2018 (IEO2018) **2018**. *2018*, 21.
3. Renewable Energies Agency. Press Fact Sheet: The German Energy Transition. *Berlin Energy Transition Dialogue* **2016**, pp. 1–16.
4. Federal Republic of Germany. Act on the Development of Renewable Energy Sources - RES Act 2017 **2017**. p. 179.
5. German Ministry of Economics and Energy. BMWi - Kraft-Wärme-Kopplung.
6. Haller, M.Y.; Haberl, R.; Mojic, I.; Frank, E. Hydraulic integration and control of heat pump and combi-storage: Same components, big differences. *Energy Procedia* **2014**, *48*, 571–580. doi:10.1016/j.egypro.2014.02.067.
7. Bloess, A.; Schill, W.P.; Zerrahn, A. Power-to-heat for renewable energy integration: A review of technologies, modeling approaches, and flexibility potentials. *Applied Energy* **2018**, *212*, 1611–1626. doi:10.1016/j.apenergy.2017.12.073.
8. Braun, J.; Bansal, P.; Groll, E. Energy efficiency analysis of air cycle heat pump dryers. *International Journal of Refrigeration* **2002**, *25*, 954–965. doi:10.1016/S0140-7007(01)00097-4.
9. Willem, H.; Lin, Y.; Lekov, A. Review of energy efficiency and system performance of residential heat pump water heaters. *Energy and Buildings* **2017**, *143*, 191–201. doi:10.1016/j.enbuild.2017.02.023.
10. Badache, M.; Ouzzane, M.; Eslami-Nejad, P.; Aidoun, Z. Experimental study of a carbon dioxide direct-expansion ground source heat pump (CO2-DX-GSHP). *Applied Thermal Engineering* **2018**, *130*, 1480–1488. doi:10.1016/j.applthermaleng.2017.10.159.
11. Ikeda, S.; Choi, W.; Ooka, R. Optimization method for multiple heat source operation including ground source heat pump considering dynamic variation in ground temperature. *Applied Energy* **2017**, *193*, 466–478. doi:10.1016/j.apenergy.2017.02.047.
12. Bacic, M. On hardware-in-the-loop simulation. *Proceedings of the 44th IEEE Conference on Decision and Control* **2005**, pp. 3194–3198. doi:10.1109/CDC.2005.1582653.
13. Bonvini, M.; Donida, F.; Leva, A. Modelica as a design tool for hardware-in-the-loop simulation **2009**. pp. 378–385. doi:10.3384/ecp09430087.
14. Bailey, M. Contributions of hardware-in-the-loop simulations to Navy test and evaluation. Proceedings of SPIE. SPIE, 1996, Vol. 2741, pp. 33–43. doi:10.1117/12.241122.
15. Winkler, D.; Gühmann, C. Hardware-in-the-Loop simulation of a hybrid electric vehicle using Modelica/Dymola. *22nd International Battery, Hybrid and Fuel Cell Electric Vehicle Symposium* **2006**, pp. 1054–1063.
16. Kamali, C.; Jain, S. Hardware in the Loop Simulation for a Mini UAV. *IFAC-PapersOnLine* **2016**, *49*, 700–705. doi:10.1016/j.ifacol.2016.03.138.
17. Sun, J.; Yin, C.; Gong, J.; Chen, Y.; Liao, Z.; Zha, X. A stable and fast-transient performance switched-mode power amplifier for a power hardware in the loop (PHIL) system. *Energies* **2017**, *10*. doi:10.3390/en10101569.
18. Guillo-Sansano, E.; Syed, M.H.; Roscoe, A.J.; Burt, G.M. Initialization and synchronization of power hardware-in-the-loop simulations: A Great Britain network case study. *Energies* **2018**, *11*. doi:10.3390/en11051087.

19. Rosa, A.; de Souza, T.; Morais, L.; Seleme, S. Adaptive and Nonlinear Control Techniques Applied to SEPIC Converter in DC-DC, PFC, CCM and DCM Modes Using HIL Simulation. *Energies* **2018**, *11*, 602. doi:10.3390/en11030602.
20. Castaings, A.; Bouscayrol, A.; Lhomme, W.; Trigui, R. Power Hardware-In-the-Loop simulation for testing multi-source vehicles. *IFAC-PapersOnLine* **2017**, *50*, 10971–10976. doi:10.1016/j.ifacol.2017.08.2469.
21. Ruuskanen, V.; Koponen, J.; Sillanpää, T.; Huoman, K.; Kosonen, A.; Niemelä, M.; Ahola, J. Design and implementation of a power-hardware-in-loop simulator for water electrolysis emulation. *Renewable Energy* **2018**, *119*, 106–115. doi:10.1016/j.renene.2017.11.088.
22. Shahid, K.; Petersen, L.; Olsen, R.; Iov, F. ICT Based HIL Validation of Voltage Control Coordination in Smart Grids Scenarios. *Energies* **2018**, *11*, 1327. doi:10.3390/en11061327.
23. Rhee, K.N.; Yeo, M.S.; Kim, K.W. Evaluation of the control performance of hydronic radiant heating systems based on the emulation using hardware-in-the-loop simulation. *Building and Environment* **2011**, *46*, 2012–2022. doi:10.1016/j.buildenv.2011.04.012.
24. El-Baz, W.; Sänger, F.; Tzscheutschler, P. Hardware in the Loop (HIL) for micro CHP Systems. *The Fourth International Conference on Microgeneration and related Technologies* **2015**.
25. Mühlbacher, H. Verbrauchsverhalten von Wärmeerzeugern bei dynamisch variierten Lasten und Übertragungskomponenten **2007**. p. 127.
26. Wehmhörner, U. Multikriterielle Regelung mit temperaturbasierter Speicherzustandsbestimmung für Mini-KWK-Anlagen **2012**.
27. Lipp, J.P. Flexible Stromerzeugung mit Mikro-KWK-Anlagen, 2015.
28. El-Baz, W.; Tzscheutschler, P.; Wagner, U. Experimental study and modeling of ground-source heat pumps with combi-storage in buildings. *Energies* **2018**, *11*. doi:10.3390/en11051174.
29. El-Baz, W.; Tzscheutschler, P. Autonomous coordination of smart buildings in microgrids based on a double-sided auction. 2017 IEEE Power & Energy Society General Meeting; IEEE: Chicago, 2017; Number August, pp. 1–5. doi:10.1109/PESGM.2017.8273944.
30. EPISCOPE. IEE Project TABULA.
31. ESI ITI. SimulationX 3.8 | Green City.
32. El-Baz, W.; Honold, J.; Hardi, L.; Tzscheutschler, P. High-resolution dataset for building energy management systems applications. *Data in Brief* **2018**, *54*, 1–5. doi:10.1016/j.dib.2017.12.058.
33. Frías-Paredes, L.; Mallor, F.; León, T.; Gastón-Romeo, M. Introducing the Temporal Distortion Index to perform a bidimensional analysis of renewable energy forecast. *Energy* **2016**, *94*, 180–194. doi:10.1016/j.energy.2015.10.093.